

TWO-DIMENSIONAL BEAM PATTERN AND PARAMETERS OF THE RATAN-600
RADIOTELESCOPE IN THE MODEL AND EXPERIMENT AT 3.2 MM WAVELENGTH

V.B. KHAIKIN, O.V. VERKHODANOV

Special Astrophysical Observatory of the Russian AS,
Nizhnij Arkhyz 357147, Russia

Received December 5, 1991

ABSTRACT. *In this paper the results of simulation of the two-dimensional beam pattern of the RATAN-600 are presented in comparison with the experiment at 3.2 mm wavelength. The antenna effective area, achieved surface accuracy $\varepsilon_{\text{surf}} = 0.25 - 0.30$ mm and main lobe efficiency of $\sim 25\%$ are calculated using integrals taken over the theoretical and experimental beam pattern. A radio image and antenna temperature expected for Jupiter at 3.2 mm are given in comparison with the the result of radio astronomical observations.*

Calculation of the two-dimensional beam pattern (BP) was carried out by the "thread-like" aperture model of Korzhavin (1977) without allowing for the finite size of the panel and its vertical illumination. This corresponds best to the field distribution in the focus measured by the method reported in (Esepkina and Petrun'kin, 1961; Khaikin et al., 1964). The field distribution in the conjugate ellipse foci lying in the horizontal plane of the VPA corresponds to its BP in the far region (FR), which is a consequence of fitting in the forms of coherent apertures at high and medium angles of observations. In both cases the apertures are approximated by a part of a circumference and though they lie in different planes.

Fig. 1 presents sections of the simulated two-dimensional BP of the RATAN-600 for a source elevation $H_0 = 63^\circ$, antenna angular aperture $\alpha = 30^\circ$, $\lambda = 3.2$ mm, and angle of horn illumination $35^\circ - 45^\circ$, corresponding to the conditions of antenna measurements (Dibizhev et al., 1990). Fig. 2a,b shows the cross-sections (horizontal, along the

x-axis) and longitudinal (vertical, along the y-axis of the computed BP, respectively. Dibizhev et al. (1990) have measured the cross-sections of the focal spot (FS) by moving the very high frequency receiver on a movable carriage in the secondary reflector focus of the RATAN-600 along the x-axis with a subsequent shift of the secondary reflector along the y-axis. The longitudinal sections were measured when the secondary reflector was moved along the y-axis. Nine cross-sections of the FS were measured in the experiment at $\lambda=3.2$ mm. Seven of them are given in Fig. 3 or on a different scale in Fig. 4. The measurements were made at the extremely short wave, $\lambda=3.2$ mm, where the effect of the reflecting surface errors, "diagonal errors", (Gosachinsky et al., 1989) and other factors distorting the FS unaccounted in the model of BP calculation become essential.

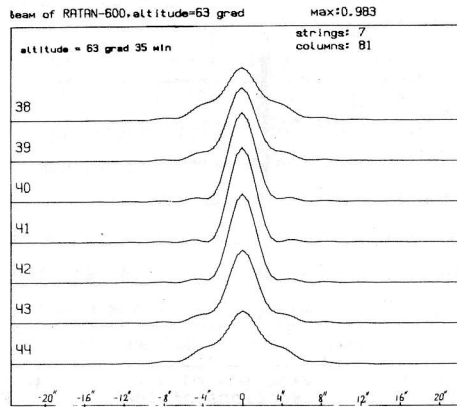


Fig. 1. Sections of calculated two-dimensional BP of the RATAN-600 radio telescope with parameters $H_0=63^\circ$, $\alpha=30^\circ$, $\varphi_{0.1}=35-45^\circ$, $\lambda=3.2$ mm.

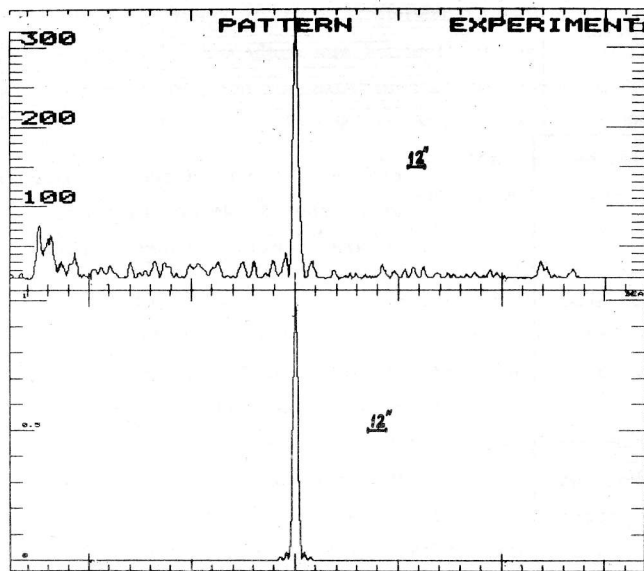


Fig. 2 a. Main cross-section of the calculated two-dimensional BP of the RATAN-600.

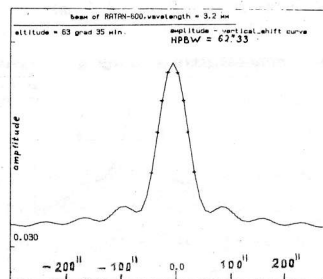


Fig. 2 b. Main longitudinal section of the calculated two-dimensional BP of the RATAN-600.

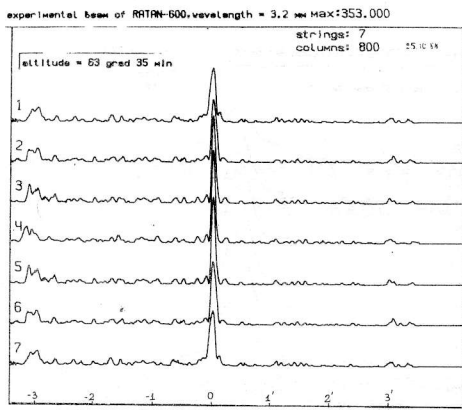


Fig. 3. Cross-sections of the measured BP at 3.2 mm.

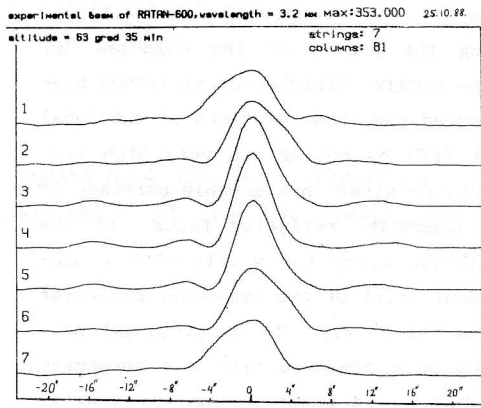


Fig. 4. Cross-sections of the measured BP at 3.2 mm on a large scale.

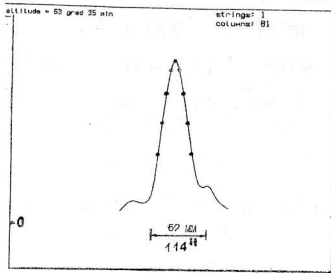


Fig. 5. Central longitudinal section of measured BP at 3.2 mm.

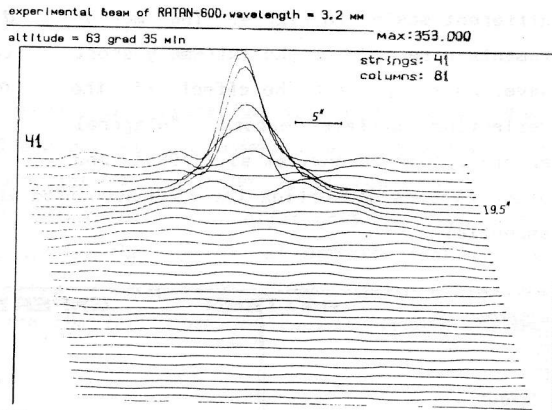


Fig. 6 a. Measured two-dimensional BP of the RATAN-600 with calculated sections added to them.

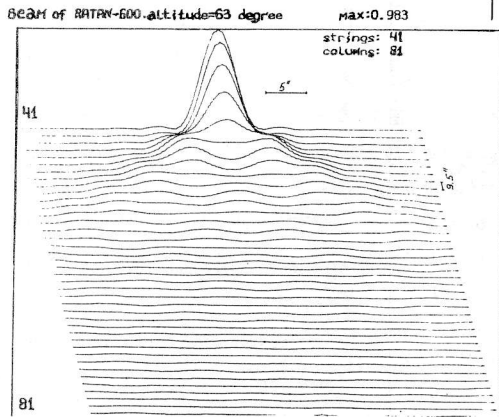


Fig. 6 b. Calculated two-dimensional BP of the RATAN-600.

Therefore the focal spot records were preceded by adjustment of the radio telescope at the wavelengths $\lambda 1.35$ cm and $\lambda 3.2$ mm with the same profile of the VPA, which reduced to minimum the position errors of the surface elements and BP distortions associated with them. Taking into account the above said for the angle $H_0 = 63^\circ$ we have a good agreement between the measured sections of the FS and the computed sections of the BP (Figs. 1, 4). Further for the sake of convenience apart from the notion of experimental FS we will use the notion of experimental BP in the same sense.

Fig. 5 presents a longitudinal section of the experimental BP, the points at which the horizontal sections of the BP were measured are also indicated here. Corresponding points are also indicated on the computed vertical BP of Fig. 2b. A comparison of the calculated and experimental sections of the two-dimensional BP, Figs. 1 and 4, 2b and 5, and the integrals taken inside and outside the region of measurements, which will be made further, allows to add the calculated sections to the measured ones as a first approximation of the experimental BP outside the region of measurements.

The procedure of adding the computed sections of the BP to the experimental ones and the need to compare the integrals of the experimental and simulated BP called for good agreement of angular scales along the longitudinal and transversal axes, and, in particular, of the step between sections of the measured and computed BP. Since the experimental BP is measured on a linear and the simulated ones on angular scales, it is necessary to bring the scales into accord. A direct recalculation of the angular scale of the computed BP into linear one will not solve the problem because the FS and BP agree with each other to an accuracy of the scale (Khaikin et al., 1964). Taking into account the extremely short wavelength, at which it is difficult to allow for all the factors that permit to represent the simulated and measured BP on one scale, this procedure was accomplished by scale fitting. For this purpose we selected a step between the experimental and computed BP ensuring their best fit.

The vertical step on the y-axis was estimated in the measured BP as follows:

1. From the amplitudes of cross-sections of the measured BP (Fig. 3) the points of the calculated two-dimensional BP were found by the least-squares method, which had the best fit to experimental. After that by averaging over the 9 points of the computed BP the step between sections on the y-axis in the experimental BP was derived.

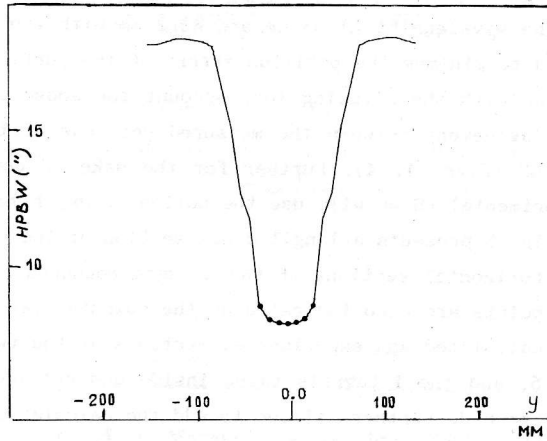
2. From the HPBW-y curve (half-width of the beam pattern of the section is a function of shift along the y-axis) presented in Fig. 7, if we know the HPBW of the measured sections, we can determine the step between the experimental sections, which is averaged over the 9 points as well.

3. From the measured half-width of the experimental vertical BP in mm (Fig. 5) with the account of the half-width of the calculated vertical BP (angular) and the known (in mm) step between the experimental sections.

All the ways gave the estimate of the step between the vertical sections to be 9-10 arcsec. Therefore in the further calculations the step between the sections $\Delta y = 9.5$ arcsec is used. The step between the samples on the x-axis in the experimental BP was

calculated as follows: the calculated BP was constructed with a number of points in the half-width equal to the number of samples in the experimental BP, from which the step between the samples $\Delta x=0.56$ arcsec followed directly.

Fig. 7. Half-width of cross-section as a function of shift along y-axis.



A fragment of the "added" BP consisting of the measured sections and calculated weighted with the help of the experimental vertical BP presented in Fig. 5 is shown in Fig. 6 a. The BP thus obtained will be called hereafter "experimental". The corresponding calculated BP is shown in Fig. 6 b.

Under the conditions of slow fall of the vertical envelope in the "thread-like aperture" model we fail to meet the requirement of convergence of the integral of this BP taken over the whole space, therefore we restrict ourselves to a certain effective integration region Ω_{eff} . Let us specify the following criterion of Ω_{eff} : a twofold increase of vertical integration region gives a 10 % rise in the integral value. A region of $45'' \times 13''$ corresponds to such a criterion of the selected parameters $H_0=63^\circ$ and illumination angle of primary feed horn $35^\circ-45^\circ$, which gives the matrix size $\Omega_{eff}=[81 \times 121]$ points if the step between the samples is $\Delta x \times \Delta y=0.56'' \times 9.5''$.

For the same reason we define the region Ω_{m1} occupied by the main lobe of the BP: assume this region as running through first zeros of the horizontal BP and through a level of 2 % of the maximum amplitude of the vertical BP. With the selected size of Ω_{eff} the matrix $\Omega_{m1}=[18 \times 81]$ points corresponds to this criterion. In this case*:

$$\frac{\iint_{\Omega_{m1}} P_{n \text{ calc}}(x, y) d\Omega}{\iint_{\Omega_{eff}} P_{n \text{ calc}}(x, y) d\Omega} = 41 \%,$$

where $P_{n \text{ calc}}(x, y)$ is the two-dimensional normalized BP of the telescope, Ω is the solid angle.

* Here and hereafter the integrals over the BP denote the sums of the kind:

$$\sum_{i=1}^n \sum_{j=1}^m P_n(x_i, y_j) \Delta x_i \Delta y_j, \text{ where } \{n, m\} \text{ data matrix dimension.}$$

Thus, in the selected model about 40 % of the energy falls within the main lobe of the BP.

To estimate the fit of the selected model to the experimental data we will use one of the main properties of the BP, "thread-like aperture" (Korzhasin, 1977): the integral taken over the cross-section of the BP does not depend in a first approximation on the distance of the given section from the center of the BP, i.e. the energy in the cross-section of the BP is preserved when moving along the y-axis:

$$\int_x P_n(x,y)dx \cong \text{const}(y). \quad (1)$$

Let us estimate the simulated and experimental BP from the point of view of the criterion mentioned.

1. Maximum difference of integrals of form (1) taken over the cross-sections of the calculated BP (Fig. 1) is $\Delta_{\text{cal}} < 0.1 \%$.

2. An averaged over the 9 cross-sections difference of integrals over the cross-sections of the experimental BP is (Fig.4) $\Delta_{\text{exp}} < 2 \%$.

Thus, the experimental BP as well as the calculated one satisfies the criterion even with the surface errors leading to the distortion of the BP at 3.2 mm. Taking into account the realization of property (1) and the analysis of the field in the region of the VPA foci made by Khaikin et al. (1964) the "thread-like aperture" model may form the basis for the calculation of the parameters of the radio telescope from the data obtained in the experiment (Dibizhev et al., 1990). However, taking into account the problem of poor convergence of integrals in the BP taken over the whole space and their replacement by integrals in a limited space region we will make the principal inferences from the ratios of integrals over the experimental and calculated BP, i.e. using the relative, but not absolute estimates for reduction of possible errors.

EFFECTIVE AREA AND PRECISION OF REFLECTING SURFACE OF THE RADIO TELESCOPE

The expected effective area of the antenna can be calculated by the formula (Christiansen and Högbom, 1988):

$$S_{\text{eff}} = \eta_r \frac{\lambda^2}{\iint_{\Omega=4\pi} P_n(x,y)d\Omega}, \quad (2)$$

where η_r is the antenna gain reflecting the internal ohmical losses in the antenna. Here and further we will take $\eta_r=0.75$ derived from the experimental data (Gosachinsky et al., 1989).

Note that the notion of effective area of the "thread-like aperture" is of condi-

tional character and is the same as effective area in the usual sense only at a finite width of the aperture and $\Omega_{\text{eff}} \rightarrow 4\pi$.

Estimate the ratio $S_{\text{eff}}^{\text{exp}}$ and $S_{\text{eff}}^{\text{calc}}$ in the region Ω_{exp} as

$$\begin{aligned}
 K_s &= S_{\text{eff}}^{\text{exp}} / S_{\text{eff}}^{\text{calc}} = \\
 &= \frac{\iint_{\Omega=4\pi} P_{\text{n calc}}(x,y) d\Omega}{\iint_{\Omega_{\text{exp}}} P_{\text{n calc}}(x,y) d\Omega + \iint_{4\pi-\Omega_{\text{exp}}} P_{\text{n calc}}(x,y) d\Omega} = \\
 &= \frac{\iint_{\Omega=4\pi} P_{\text{n exp}}(x,y) d\Omega}{\iint_{\Omega_{\text{exp}}} P_{\text{n exp}}(x,y) d\Omega + \iint_{4\pi-\Omega_{\text{exp}}} P_{\text{n exp}}(x,y) d\Omega} = \\
 &= \frac{\iint_{\Omega_{\text{exp}}} P_{\text{n calc}}(x,y) d\Omega (1+I_1)}{\iint_{\Omega_{\text{exp}}} P_{\text{n exp}}(x,y) d\Omega (1+I_2)}, \quad (3)
 \end{aligned}$$

where

$$\begin{aligned}
 I_1 &= \frac{\iint_{4\pi-\Omega_{\text{exp}}} P_{\text{n calc}}(x,y) d\Omega}{\iint_{\Omega_{\text{exp}}} P_{\text{n calc}}(x,y) d\Omega}, \\
 I_2 &= \frac{\iint_{4\pi-\Omega_{\text{exp}}} P_{\text{n exp}}(x,y) d\Omega}{\iint_{\Omega_{\text{exp}}} P_{\text{n exp}}(x,y) d\Omega}.
 \end{aligned}$$

It is clear that to obtain $I_1, I_2 \ll 1$ one has to choose the region Ω_{exp} in which a considerably larger part of energy is concentrated as compared to the region $4\pi - \Omega_{\text{exp}}$. In our case this is valid for the region $\Omega_{\text{exp}} = \Omega_{\text{eff}}$.

$$K'_s = \frac{\iint_{\Omega_{\text{eff}}} P_{\text{n exp}}(x,y) d\Omega}{\iint_{\Omega_{\text{eff}}} P_{\text{n calc}}(x,y) d\Omega} \quad (4)$$

The loss of the BP energy contained in the region $4\pi - \Omega_{\text{eff}}$ will lead to the majorant character of the estimate $K'_s > K_s$, which in turn provides a lower limit to possible surface errors and $K'_s \rightarrow K_s$ at $\Omega_{\text{eff}} \rightarrow 4\pi$.

As a result of computing K' by formula (4) we obtain $K' = 0.46$.

Assuming that the whole drop in the effective area is due to random surface errors

ϵ_{surf} :

$$K' = e^{-\frac{(4\pi\epsilon_{\text{surf}}/\lambda)^2}{2}}$$

obtain $\epsilon = 0.22$ mm.

The derived value is a lower estimate as the derivative of the majorant K'_s . Besides, Dibizhev et al. (1990) measured the focal field at the vertical position of the antenna elements, which did not allow for additional errors arising when setting the elements to a cosmic source. Evaluating a contribution of the error mentioned for

the observational angle $H_0 = 63^\circ$ as $\Delta\varepsilon = 0.10-0.15$ mm, which follows from the data of geodesic measurements, we obtain the estimate of the surface error in the working position of the antenna to be $\varepsilon_{\text{surf}} = 0.24-0.27$ mm. In the obtained $\varepsilon_{\text{surf}}$ the surface error of an individual element introduces integral contribution, i.e. it is averaged vertically for every element of the "thread-like aperture", which also characterizes $\varepsilon_{\text{surf}}$ as the lower limit of possible error. The allowance for the surface error of the secondary reflector $\sigma = 0.12$ (Zverev and Golosova, 1989) estimates the error of the focusing system $\varepsilon_{\text{foc}} = 0.27-0.30$ mm.

Calculate S_{eff} with the account of the derived estimate of ε_{foc} and the known geometrical area of the antenna:

$$S_{\text{eff}} = S_{\text{geom}} \eta_v \eta_h \eta_r \eta_d \exp\{-(4\pi\varepsilon_{\text{foc}}/\lambda)^2\},$$

in our case S_{geom} is 150×1.5 m (75 elements with partial vertical illumination were used in the measurements).

The coefficients η_h , η_v are related to horizontal and vertical illumination of the surface, respectively, η_r reflects ohmical losses in the antenna, η_d is caused by "diagonal errors" of the antenna at 3.2 mm.

Make use of the results of evaluation the indicated coefficients obtained in (Gosachinsky et al., 1989) for the same antenna size, primary horn, and wavelength:

$\eta_v = 0.8$; $\eta_h = 0.81$; $\eta_r = 0.77$; $\eta_d = 0.94$. Then we obtain $S_{\text{eff}} = 25-35$ m². The similar estimate of S_{eff} was obtained in (Gosachinsky et al., 1989). However, in our case the antenna adjustment and subsequent measurements of the BP were performed at one and the same antenna position. The estimate of the total surface error $\varepsilon_{\text{surf}} = 0.3$ mm, presented in the paper mentioned seems to us too optimistic since from the data of (Dibizhev et al., 1990) only the error of antenna transition from autocollimation position, at which the alignment of surface elements (Venger et al., 1989) to the working profile was performed is $\varepsilon_{\text{trans}} = 0.25-0.35$ mm.

ENERGY IN THE MAIN LOBE OF BP

The experimental BP presented in Fig. 3 does not contain noticeable scattering backgrounds. Their contribution can be more efficiently estimated from observations of extended sources, in particular by the Moon, which was done in (Gosachinsky et al., 1989). However, we will estimate the energy concentrated in the main lobe of the experimental BP since in the absence of strong point sources in the wavelength range in question, the corresponding estimates made from extended objects do not provide a high accuracy due to the contribution of the scattering background of different scales and convolution of the BP with the surface brightness distribution of the source.

In correspondence with the previously established notion of the main lobe of the

BP we obtain the estimate:

$$\iint_{\Omega_{m1}} P_{n \text{ exp}}(x, y) d\Omega / \iint P_{n \text{ exp}}(xy) d\Omega \approx 25 \%$$

Thus, the portion of energy in the main lobe of the experimental BP immediately after the adjustment of the antenna with the working profile is 25 %, which is approximately 60 % of the computed energy with the allowance for the selected model.

EXPECTED ANTENNA TEMPERATURE OF JUPITER AT 3.2 MM

According to the equation of antenna smoothing:

$$T_a = \frac{\eta_r \iint_{\Omega_s} P_n(x, y) T_{br}(x, y) d\Omega}{\iint_{\Omega=4\pi} P_n(x, y) d\Omega} \quad (5)$$

where T_a and T_b are the antenna and brightness temperatures of the source, Ω_s is the solid angle of the source.

Compute the convolutions of the kind $P_n(x, y) \times T_b(x, y)$ to obtain the expected radio image of Jupiter and to estimate its antenna temperature. Figs. 8, 9 present the results of the procedure for the calculated and experimental BP. As the model of Jupiter a disc of 40" in diameter was used with a "table-like" distribution of surface brightness and $T_{bJ} = 170$ K at the wavelength 3.2 mm, which simulated the conditions of Jupiter observation in the given period. Fig. 10a, b shows for comparison

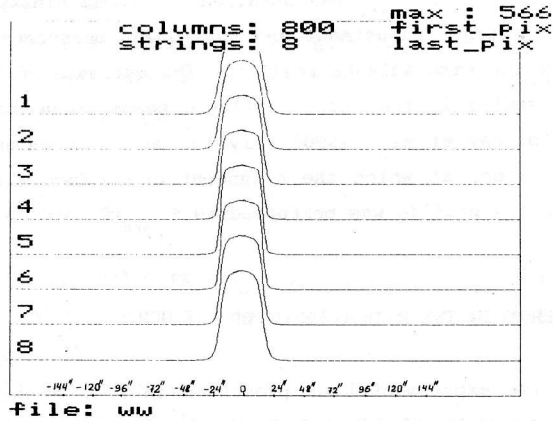


Fig. 8. Convolution of the calculated BP of the RATAN-600 at 3.2 mm.

the central sections of the expected radio response of the antenna to Jupiter passage for the computed and experimental BP. Fig. 10 c, d presents the central sections of the calculated and experimental BP. Fig. 10 b' shows the curve of Jupiter transit in a real radio astronomy experiment averaged over 6 records (Gosachinsky et al., 1989).

The central section of the expected response of Jupiter constructed on the same scale from the experimental BP is shown in Fig.10 b''. The anomalous response of the antenna in the left part of Fig.10 b and the corresponding response of BP (Fig.10 d) on the scale of the order of surface element is caused by large systematic and random azimuth errors of antenna (Dibizhev, et al., 1989). Despite the correction of the antenna profile in the process of adjustment we failed to eliminate completely the contribution of these errors because of the large azimuth clearance, though their influence was greatly reduced.

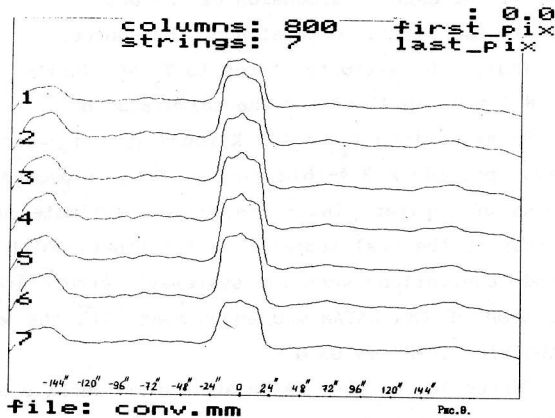


Fig. 9. Convolution of experimental BP of the RATAN-600 at $\lambda 3.2$ mm with simulated Jupiter disc.

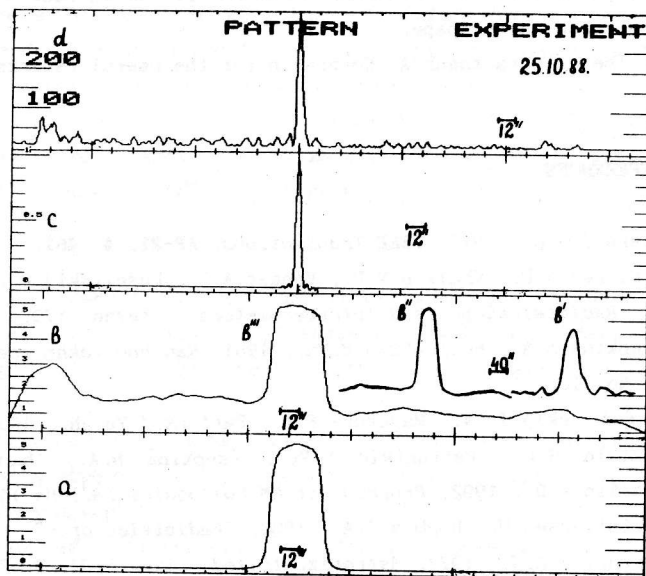


Fig. 10 a-d. Expected and observed radio images of Jupiter:
a - expected antenna response for calculated BP of the RATAN-600;
b - expected antenna response for experimental BP of the RATAN-600;
c, d - central sections of calculated and experimental BP of the RATAN-600.

The computation of the antenna temperature of Jupiter T_{aJ} by formula (4) using the experimental and calculated BP yields $T_{a \text{ exp}} \approx 3$ K and $T_{a \text{ calc}} \approx 6$ K, respectively,

which does not exceed 4 % of the Jupiter's brightness temperature.

Compare the derived estimate of T_a of Jupiter with the appropriate estimate in (Gosachinsky et al., 1989) by the formula from (Baars, 1973):

$$T_a = \eta_r \exp(\delta)^2 T_{br} / (g \Omega_0 / \Omega_1),$$

where $\delta = 4\pi\varepsilon/\lambda$,

ε is the root-mean-square error of the surface,

Ω_0 is the angular dimension of the BP,

Ω_1 is the angular dimension of the source.

Thus, the estimate tends to T_a of Jupiter, 7-10 K which is close to the value $T_a \approx 6$ K we obtained for the calculated BP.

So at maximum $T_{aJ} = 1.9$ K found in the experiment (Gosachinsky et al., 1989) both ways provide a 3-4-fold excess of the expected calculated and real antenna temperatures of Jupiter. The corresponding estimate of T_{aJ} from the experimental BP also surpasses the real temperature 1.5 times, which allows to expect a rise of S_{eff} in mm band observations when the systematic errors are eliminated and the radio holography method of the RATAN-600 adjustment with the working profile of the main reflector (Khaikin, 1992) is used.

Correction of systematic and random surface errors distorting the BP of the RATAN-600 and extension of the region of Ω_{exp} measurements allows to specify in the future the parameters of the radio telescope in the mm band with the help of the technique described in the paper.

The authors thank A. Korzhavin for the useful remarks made in the process of work.

REFERENCES

- Baars J.W.M.: 1973, *IEEE Transactions*, AP-21, 4, 461.
- Dibizhev A.D., Khaikin V.B., Venger A.P., Loshitskij P.P.: 1990, *All-union Conference "Radiotelescopes and interferometers"*, Erevan, 170.
- Esepkina N.A., Petrun'kin V.Yu.: 1961, *Nauchno-tehnicheskij Byul. LPI, Radiofizika*, No. 10.
- Gosachinskij I. V., Majorova E.K., Parijskij Yu. N.: 1989, *Soobshch. SAO*, 63, 38.
- Khaikin S.E., Petrun'kin V.Yu., Esepkina N.A., Umetskij V.N., Kuznetsov V.G., Khaikin V.B.: 1992, *Proceed. of MM Colloquium IAU*, No 140, Hakone, Japan.
- Khristiansen U., Högbom J.A.: 1988, *"Radiotelescopes"*, M: Mir.
- Korzhavin A.N.: 1977, *Astrofiz. Issled. (Izv. SAO)*, 9, 71.
- Vasil'ev B.A.: 1964, *Izv. GAO*, 172, 128.
- Venger A.P., Dibizhev A.D., Pinchuk G.A., Sinyanskij V.I., Plyaskin S.P.: 1989, *Soobshch. Spets. Astrofiz. Obs.*, 63, 18.
- Zverev Yu.K., Golosova S.Ya.: 1989, *Soobshch. Spets. Astrofiz. Obs.*, 63, 8.